Functional Materials 13, No.2 (2006)

Foreign phase inclusions in Ti-sapphire grown in a carbon-containing medium

S.D.Vyshnevskiy, Ye.V.Kryvonosov, L.A.Lytvynov

Institute for Single Crystals, National Academy of Sciences of Ukraine,
60 Lenin Ave., 61001 Kharkiv, Ukraine

Received October 19, 2005

The effect of carbon-containing growth medium on the character and formation features of foreign phase inclusions in Ti-sapphire has been studied. The crystals so grown may include both micrometer-sized (2 to 17 μm) and submicrometer-sized (about 100 nm) inclusions. The specifically cut micrometer-sized inclusions have been shown to be pores. The shape and orientation of submicrometer-sized inclusions in Ti-sapphire have been studied. A formation mechanism has been suggested for submicrometer-sized inclusions containing excess aluminum ant its suboxides. The inclusions are formed in solid phase in the course of phase transition at the crystallization front as a result of the crystal lattice supersaturation with anionic vacancies. Those defects are collapsed under the crystal high-temperature heat treatment due to uniaxial compressive stresses.

Исследовано влияние углеродосодержащей среды выращивания на характер и особенности формирования инофазных включений в Ti-сапфире. Установлено, что эти кристаллы могут содержать: микронные (2...17 мкм) и субмикронные (около 100 нм) включения. Показано, что микронные включения, имеющие характерную огранку, являются порами. На основании индикатрис оптического рассеяния исследована форма и ориентация субмикронных включений в Ti-сапфире. Предложен механизм формирования субмикронных включений, содержащих избыточный алюминий и его субокислы. Включения формируются в твёрдой фазе в процессе фазового перехода на фронте кристаллизации как результат пересыщения кристаллической решётки анионными вакансиями. Эти дефекты разрушаются в результате высокотемпературной термообработки кристаллов под действием одноосных сжимающих напряжений.

The α-Al_2O_3:Ti^{3+} (Ti-sapphire) crystals are used as active medium for frequency-tunable solid-state lasers. The foreign phase inclusions deteriorate considerably the performance characteristics of a laser crystal due to increased optical losses and decreased radiation stability of the crystal. The inclusion formation is influenced by the growing medium that changes the physicochemical crystallization conditions and the melt stoichiometry [1]. The Ti-sapphire is grown by Czochralsky technique and using the HEM (heat exchange method), VSOM (vertical solidification of the melt), IFSM (induction field up-shift method) from iridium and molybdenum crucibles under reducing atmosphere containing argon and hydrogen [2–4]. Using graphite heaters and graphite-containing heat-insulating materials provides a carbon-containing crystallization atmosphere having a high reducing potential [5]. In leukosapphire grown by horizontal directional crystallization (HDC) and IFSM in a carbon-containing medium, cut foreign phase micro-inclusions have been found. There are various viewpoints as to the nature and formation mechanism of those inclusions. These are supposed to be molybdenum particles formed due to melt interaction with the crucible material caused by free oxygen presence in the melt or in growth gas medium [6]. The cut inclusions, according to [7], are AlO–Al_2O_3 (Al–Al spinel) particles formed in the melt ahead

of the crystallization front. This phenomenon is due to the melt deviation from the stoichiometry caused by the high reducing chemical potential of the crystallization medium. The inclusion of 0.5 to 5 μm inclusions are micrometer-sized gas bubbles captured by the crystal out of the melt that has lost the overcooling resistance due to the reducing crystallization medium [8]. The technology features and optical properties of crystals grown by Czochralsky technique in a carbon-containing medium have been studied in [9]. It is just the Tyndall light scattering on the 2 to 10 μm size gas microinclusions that limits mainly the optical quality of the crystals. The formation mechanism of the optical scattering centers in those crystals was not considered up to now. This work is aimed at the study of the carbon-containing medium on the character and formation features of foreign phase inclusions in Ti-sapphire grown by Czochralsky technique.

The Ti-sapphire (Ti^{3+} content 0.06 to 0.12 % wt) was grown by Czochralsky technique from a molybdenum crucible in a Krystall-3M unit with a graphite heater. Argon (730 to 920 Torr) was used as the protecting atmosphere. The crystals were grown along the [11$\bar{2}$0] crystallographic direction. The Verneuil-grown sapphire breakage and titanium dioxide were used as initial materials. The grown crystals were annealed in vacuum ($2 \cdot 10^{-4}$ Torr) at 1980°C without loading as well as under uniaxial compressive stress of $7.8 \cdot 10^5$ N/m^2. The optical absorption spectra were measured using 1.5 mm thick samples cut out perpendicular to the growth direction. The foreign phase inclusion distribution was studied using optical microscopy and light scattering.

In Ti-sapphire grown by Czochralsky technique in a carbon-containing medium, foreign phase inclusions various in the shape and size may exist, depending on the crystallization conditions: gas-filled inclusions (pores and voids) of 12 μm to several millimeters size; cut inclusions of 2 to 17 μm size; and sub-micrometer inclusions (about 100 nm).

Basing on consideration of more than 100 crystals, a regularity has been established in the inclusion distribution along the ingot length. In the seed-close area, the gas-filled inclusions are localized as a rule. As the distance from the seed increases, the cut inclusions may arise. Then an inclusion-free area is located. At the crystal end, an area containing the sub-micrometer inclusions is formed. The size of each area containing the specific inclusion types depends on the crystallization conditions, but the sequence thereof along the ingot remains the same. Moreover, several defect types may coexist in one and the same crystal part.

The gas-filled inclusions are often observed as the crystal grows from a gas-saturated melt. The gas bubbles in the melt arise due to gases adsorbed at the crucible surface, volatile impurities in the raw material as well as the thermal dissociation of the melt itself. The gas bubbles can be formed at active centers (microcracks, open micropores) of the crucible inner surface that heats the melt [10]. In this case, no significant supersaturation of the melt by a gaseous impurity is needed, because the gas is released into an existing gas bubble. At the initial crystallization stage, the melt may contain a considerable amount of gas bubbles. In this case, separate inclusions of 0.1 to 2 mm size are formed in Ti-sapphire as well as characteristic gas voids up to several tens of millimeters in size.

As corundum is crystallized in a carbon-containing medium, the melt becomes depleted of oxygen; that is equivalent to an excess aluminum content in the melt. This is due to interaction of carbon oxide in the gas medium with oxygen arising due to thermal dissociation of Al_2O_3 [11]. Ti-sapphire grown in those conditions contains cut inclusions of 2 to 17 μm size (Fig. 1). Such inclusions were observe also in sapphire grown by HDC method [7]. The cut inclusions decorate the crystallization front at the growth speed fluctuations; this evidences the localization thereof in the melt at the crystal surface. If the cut micrometer-sized inclusions are supposed to be molybdenum particles, then the concentration thereof should increase as the reducing chemical potential of the crystallization medium drops and the free oxygen amount in the melt increases. However, no cut micrometer-sized are observed in Ti-sapphire grown using Kyropoulos technique in a W–Mo thermal assembly at neutral chemical potential of the crystallization medium. Moreover, the atomic emission spectral analysis of the residual melt after Ti-sapphire growing in carbon-containing medium did not shown any considerable increase of the molybdenum content as compared to the initial material (see Table 1). Thus, there is no appreciable interaction between the melt and the container material. Besides, the concentration of molybdenum inclusions

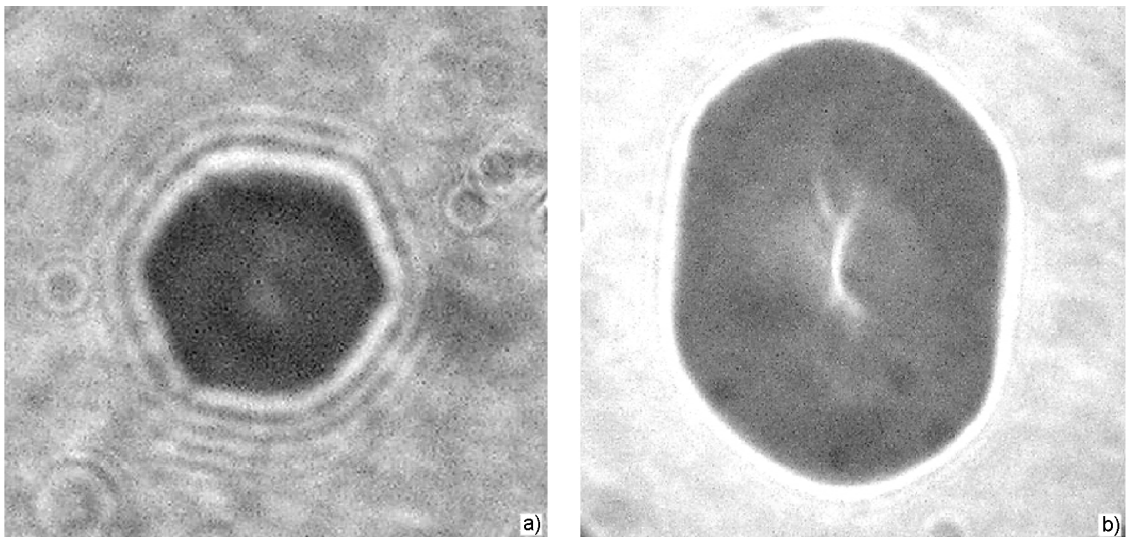

Fig. 1. Cut (a) and partially cut (b) inclusion of 17 and 40 μm size, respectively, in Ti-sapphire.

must increase at the crystallization end, that does not correspond to the distribution character of the cut inclusions over the crystal length. Thus, the cut micrometer-sized inclusions in the crystal are not the crucible material particles.

Formation of $AlO{\cdot}Al_2O_3$ solid phase particles at the crystallization front is also unlikely, since the melting point of $AlO{\cdot}Al_2O_3$ spinel is 1980 to 1990°C [12], thus excluding the formation of those particles in the aluminum oxide melt having a temperature about 2050°C. Moreover, the solid-phase inclusions based on impurity/vacancy complexes in corundum crystals have been shown to be effectively destroyed at high-temperature annealing [13, 14]. The vacuum annealing eliminates the excess anionic vacancies in the crystal lattice and thus must favor the destruction of solid-phase $AlO{\cdot}Al_2O_3$ spinel inclusions being formed due to excess aluminum atoms in the corundum lattice. However, the cut inclusions are not disappear after the Ti-sapphire is heat-treated in vacuum for 40 h at 2000°C. Thus, the cut micrometer-sized inclusions in the crystal are not the solid-phase formations based on excess aluminum.

Table 1. Chemical composition of raw material, crystal, and residual melt after crystallization

Sample	Element content, ppm					
	Fe	Ca	Mg	Si	Mo	W
Raw material	10	<5	3	20	<0.5	<10
Crystal	4	5	1	10	5	<10
Residual melt	10	150	3	10	3	25

In our opinion, it is quite possible that the cut micrometer-sized inclusions are formed in the melt as gas bubbles captured by the crystal in growth, as has been supposed in [8]. The individual bubbles can be captured by the crystal without the morphologic stability loss of the crystallization front [15]; this fact can explain the presence thereof outside the mass capture zone. It explaines also the insensibivity of those defects to the high-temperature vacuum annealing. A gas bubble in the melt contains, along with the dissolved gases released thereto, the vapors formed due to Al_2O_3 chemical dissociation. The partial pressure of those vapors depends on the melt deviation from stoichiometry [16]. Graphite, being used as a heater, creates a high reductive chemical potential ε (−190 to −230 kJ/mol) in the crystallizer operating space, that results in the melt deviation from stoichiometry and its supersaturation with aluminum atoms. This process is also favored by the displacement of the excess aluminum by the crystallization front. As a result, conditions corresponding to the $Al–Al_2O_3$ system may become realized in the melt. The gas phase of that system contains two main components (Al, 12.8 % and Al_2O, 87 %), the total pressure thereof in the 2327–2500 K temperature interval is defined by the relationship (2) and may attain 1.7 atm [16]:

$$\lg \sum P_{(Al–Al_2O_3)} = -16308/T + 6.775. \quad (2)$$

Table 2. 90° scattering as a function of crystallographic direction

Laser beam propagation direction	Scattering record direction	90° scattering intensity (a.u.)
[11$\bar{2}$0]	[1$\bar{1}$00]	24.7
	[0001]	7,3
[1$\bar{1}$00]	[11$\bar{2}$0]	24.4
	[0001]	7.1
[0001]	[11$\bar{2}$0]	8.7
	[1$\bar{1}$00]	8.6

Thus, gas bubbles with a high content of Al and Al_2O components may be formed in a melt deviated from stoichiometry. After these bubbles are captured by the crystal, the vapors contained therein are condensed and the pressure within the bubble drops. As a result of the material diffusion, the bubbles are transformed into cut pores with cutting being defined by the corundum single crystal morphology [17], elastic stresses in the crystal lattice, structure defects in the pore nearest surrounding and the impurity localization near its surface. The pore cutting is favored also by its prolonged presence in the "hot" post-crystallization thermal zone. This inclusion formation mechanism is supported by a pronounced cutting in the pores of less than 17 μm size and a partial cutting of larger (20 to 50 μm) inclusions (Fig. 1). The phenomenon is explained by the fact that the Laplacian pressure depends on the inclusion size.

Under some conditions, sub-micrometer size inclusions are formed in Ti-sapphire grown in carbon-containing medium. These inclusions are destroyed by high-temperature vacuum annealing. Those are invisible under an optical microscope but cause a Tyndall scattering of a He–Ne laser beam. As the non-polarized laser beam passes through the crystal, the light scattered at 90° to the incident beam direction is polarized linearly. This evidences the sub-micrometer size of the inclusions (about 100 nm) [19]). Intensity of such scattering depends on the crystallographic direction (see Table 2); this is typical of non-spherical shape of the sub-micrometer inclusions and their uniform orientation in the crystal. As a first approximation, the non-spherical particles can be presented as ellipsoids of revolution. Under Rayleigh-Hans approximation, the intensity of light scattered at the angle β is [19]

$$I_S = I_R \cdot [F(\beta,\Delta)]^2, \qquad (3)$$

where I_R is the Rayleigh light scattering; $F(\beta,\Delta)$, the phase function depending on the scattering angle, the particle size and position. For particles of a size much smaller than the incident light wavelength,

$$F(\beta,\Delta) = \left[\frac{1-\varepsilon^2}{1-\varepsilon^2+\alpha^2(1-\alpha^2)\varepsilon^4}\right]^{\frac{3}{2}} \times \times\left[1+\frac{3}{2}\cdot\frac{\alpha^2(1-\alpha^2)\varepsilon^4}{1-\varepsilon^2}\right], \qquad (4)$$

where $\alpha = (\cos\Delta - R_{0x})/2\sin(\beta/2)$; Δ, the angle between the ellipsoid symmetry axis and the incident light propagation direction; R_{0x}, the projection of unit vector R_0 (directed from the center of the scattering particle to the observation point) on the ellipsoid symmetry axis; ε, the ellipsoid excentricity.

As the laser beam passes the sample along the crystal optical axis, the 90° scattering intensity is the same in all the directions. Thus, the symmetry axis of ellipsoid approximating the submicrometer-sized inclusion coincides with the crystal optical axis. Using the scattered light intensity ratio for two different orientations I_{1s}, I_{2s} of a particle with respect to the incident light wave,

$$I_{1s}/I_{2s} = [F(\beta,\Delta)_1/F(\beta,\Delta)_2]^2 \qquad (5)$$

and proceeding from the experimental data (Table 2), one axis of the ellipsoid can be estimated to be 5 times longed than another one.

Corundum single crystals grown in carbon-containing medium and containing the submicrometer-sized inclusions are characterized by a high concentration of anionic vacancies ($2\cdot10^{17}$ cm^{-3}) [5], as is indicated by optical absorption at 206, 225, and 268 nm [20, 21]. The vacancy concentration in the crystal area containing the submicrometer-sized inclusions exceeds that in defect-free area (Fig. 2). At the other hand, Ti-sapphire grown in graphite-free Mo–W thermal assemblies does not contain the submicrometer-sized inclusions. The optical absorption spectrum of such crystals is characterized by a broad UV absorption band peaked at 220 nm, thus evidencing an excess of cationic vacancies in the crystal lattice [22].

The submicrometer-sized inclusions are formed along the (0001) planes and their distribution is characterized by an oriented

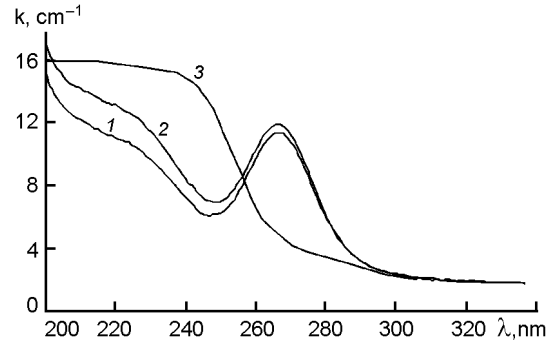

Fig. 2. UV absorption spectra for Ti-sapphire grown in a carbon-containing medium (*1*, *2*) and in a W–Mo thermal assembly (*3*). Defect-free crystal area (*1*) and that containing submicrometer inclusions (*2*).

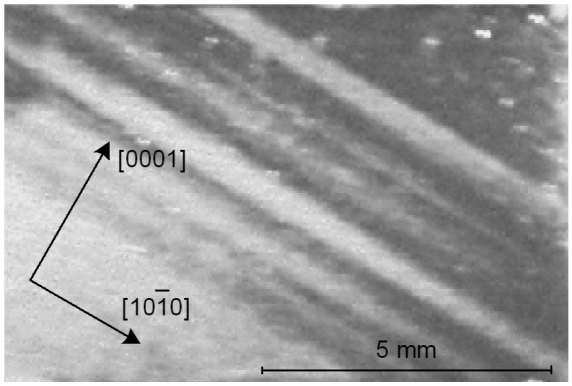

Fig. 3. Striate-like distribution of submicrometer inclusions in Ti-sapphire.

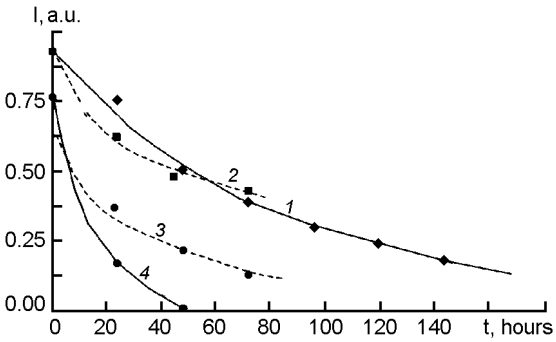

Fig. 4. Destruction dynamics of submicrometer inclusions at Ti-sapphire vacuum annealing without loading (*1*) and under uniaxial compressive stress $\sigma = 7.8 \cdot 10^5$ N/m^2 applied along different crystallographic directions: [11$\bar{2}$0] (*2*), [0001] (*3*), [1$\bar{1}$02] (*4*).

striation that is not associated with the crystallization front shape (Fig. 3). This evidences the formation of the submicrometer-sized inclusions in the solid phase behind the crystallization front or directly at the front during the melt-crystal phase transition. It seems that it is just the excess anionic vacancies and aluminum ions that give rise to submicrometer-sized inclusions in corundum. Due to coagulation of anionic vacancies, the submicrometer-sized inclusions of a foreign phase are formed in the crystal; the inclusions contain an excess of aluminum and its suboxides that are condensed during cooling at the inner surface of submicrometer pores. This explains the increased concentration of anionic vacancies in the crystal area containing the submicrometer-sized inclusions. As to leuko-sapphire, the submicrometer-sized inclusions are formed only seldom in similar conditions. Their generation in Ti-sapphire seems to be favored by the activator ions (Ti^{3+}) with ionic radius (0.69 Å) exceeding that of aluminum (0.57 Å). The impurity ions cause local stresses in the crystal lattice, thus lowering the formation work of the submicrometer-sized inclusion critical nucleus.

The vacuum annealing of Ti-sapphire results in diffusion of the anionic vacancies from the matrix and dissolution of aluminum atoms (being contained in the submicrometer-sized inclusion) in the crystal matrix. At a certain annealing stage, those inclusions become transformed into submicrometer pores containing saturated aluminum oxide vapor. The pores in a crystal are known to be diffusively dissolved [23] or to be cured according to the dislocation mechanism [24]. The diffusive dissolution of a pore is due to an increased vacancy concentration at its surface. In its turn, a constant uniaxial load applied to the crystal favors the diffusion processes and the diffusion-dislocation creeping, thus increasing the pore dissolution rate [25]. The destruction dynamics of the submicrometer-sized inclusions in the crystal was monitored using the decrease of optical scattering intensity that is in proportion to the scattering center concentration [19].

The dislocations in corundum single crystals show a maximum mobility under cleaving stresses directed along the (0001) plane belonging to the easiest sliding system [18]. Under uniaxial stresses along the [11$\bar{2}$0] and [0001] directions, those cleaving stresses are minimal, the dislocation motion in the (0001) plane is hindered, and the pore is cured mainly due to the vacancy-by-vacancy dissolution. This is confirmed by the fact that the submicrometer-sized inclusions are dissolved at the same rate during the sample annealing without any loading

and under uniaxial compressive stresses acting along [11$\bar{2}$0] and [0001] (Fig. 4). The submicrometer pores are destroyed most intensely at the high-temperature vacuum annealing of the crystal under uniaxial compressive stresses applied along the [1$\bar{1}$02] crystallographic direction, since in this case, both mechanisms of pore dissolution are active.

Thus, the cut micro-inclusions in Ti-sapphire grown in a carbon-containing medium are pores. Gas bubbles of micrometer size with a high Al and Al_2O vapor concentration are formed in the melt and are captured by the crystal in growth. Due to vapor condensation inside the captured bubbles and the material diffusion flowing in the nearest surrounding thereof, the cut inclusions of 2 to 17 μm size are formed in the crystal. The sub-micrometer size inclusions in Ti-sapphire are formed in the solid phase in the course of phase transition at the crystallization front as a result of the crystal lattice supersaturation with aluminum ions and anionic vacancies. The anionic vacancy coagulation gives rise to sub-micrometer size (about 100 nm) inclusions containing aluminum and its suboxides are formed in the crystal. The inclusion generation is favored by titanium ions and unintentional impurity ones. The crystal high-temperature annealing in vacuum under uniaxial compressive stresses favors the destruction of sub-micrometer size inclusions but does not influence the cut ones. The annealing efficiency is defined by the applied loading direction.

References

1. A.A.Chernov, E.I.Givargizov, Kh.S.Bagdasarov et al., Modern Crystallography, Vol.3 (Crystal Formation), Nauka, Moscow (1980) [in Russian].
2. P.Lacovara, L.Esterovitz, M.Kokta, *IEEE J. of Quantum Electronics*, **QE-21**, 1611 (1985).
3. R.C.Powell et al., *J.Appl.Phys.*, **58**, 2331 (1985).
4. Deng Peizden et al., *Proc.SPIE*, **1338**, 207 (1990).
5. E.V.Krivonosov, *Functional Materials*, **1**, 105 (1994).
6. M.I.Musatov, in: Physics of Crystallization, Kalinin (1986), p.43 [in Russian].
7. A.Ya.Dan'ko, N.S.Sidelnikova, G.T.Adonkin et al., *Kristallografia*, **49**, 294 (2004).
8. A.L.Samsonov, T.S.Bessonova, S.V.Bodyachevsky, *Optiko-Mekhan.Prom.*, **6**, 60 (1991)
9. E.V.Krivonosov, L.A.Lytvynov, *Functional Materials*, **3**, 77 (1996).
10. E.I.Nesis, Boiling of Liquids, Nauka, Moscow (1973) [in Russian].
11. V.S.Konevsky, E.V.Krivonosov, L.A.Litvinov, *Izv.AN SSSR, Ser.Neorg.Mater.*, **25**, 1486 (1989).
12. N.E.Filonenko, I.V.Lavrov, O.V.Andreeva, R.L.Pevzner, *Dokl.AN SSSR*, **115**, 583 (1957).
13. Ye.V.Kryvonosov, L.A.Lytvynov, S.D.Vyshnevskiy, *Journal of Crystal Growth.*, **275**, 691 (2005).
14. I.A.Zhizheiko, V.Ya.Khaimov-Malkov, *Kristallografia*, **23**, 1227 (1978).
15. A.A.Chernov, D.E.Temin, A.M.Melnikov, *Kristallografia*, **21**, 652 (1976).
16. A.L.Samsonov, S.V.Bodyachevsky, *Izv.AN SSSR, Ser.Neorg.Mater.*, **24**, 1666 (1988).
17. W.C.Mackrodt, R.J.Davey, S.M.Black, *Journal of Crystal Growth.*, **80**, 441 (1987).
18. M.V.Klassen-Neklyudova, Kh.S.Bagdasarov, Ryby and Sapphire, Nauka, Moscow (1974) [in Russian].
19. K.S.Shifrin, Light Scattering in Turbid Media, Izdat. Tekhn.-Teor. Liter., Moscow (1951) [in Russian].
20. B.D.Evans, B.Stapelbrock, *Phys.Rev.B.*, **18**, 7089 (1978).
21. V.S.Konevsky, E.V.Krivonosov, L.A.Litvinov, M.I.Shakhnovich, *Zhurnal Prikladnoy Spektroskopii*, **50**, 651 (1988).
22. E.M.Akul'onok, V.Ya.Khaimov-Mal'kov, Yu.K.Danileiko et al., *Journal of Solid State Chemistry*, **26**, 17 (1978).
23. Ya.E.Geguzin, I.M.Lifshits, *Fiz.Tverd.Tela*, **4**, 1326 (1962).
24. Ya.E.Geguzin, V.G.Kononenko, *Fiz.Khim. Obrab.Mater.*, **2**, 60 (1982).
25. L.A.Shuvalov, A.A.Urusovskaya, I.S.Zheludev, Modern Crystallography, Vol.4 (Physical Properties of Crystals), Nauka, Moscow (1981) [in Russian].

Інофазні включення в Ti-сапфірі, що вирощено у вуглецевому середовищі

С.Д.Вишневський, Е.В.Кривоносов, Л.А.Литвинов

Досліджено вплив вуглецевого середовища кристалізації на характер і особливості утворювання інофазних включень в Ti-сапфірі. Встановлено, що ці кристали можуть містити: мікронні (2 17 мкм) і субмікронні (менше 70 нм) включення. Показано, що мікронні включення є порами і мають характерне огранування. На підставі аналізу індікатріси оптичного розсіяння досліджена форма і орієнтація субмікронних включень в Ti-сапфірі. Запропоновано механізм формування субмікронних включень, які є зародками пор і утворюються в твердій фазі в процесі фазового переходу на фронті кристалізації як результат пересищення кристалічної решітки аніонними вакансіями. Встановлено, що ці дефекти руйнуються в результаті високотемпературної термообробки кристалів під дією одноосних стискуючих напруг.